Turk J Elec Engin, VOL.11, NO.1 2003, © TÜBİTAK

# Resonant Demagnetization PWM Forward Converter

**Bülent BİLGİN**
*Aselsan Inc., PK-101, Ankara-TURKEY*
**Işık ÇADIRCI, Rüyal ERGÜL and Muammer ERMİŞ**
*METU Electrical and Electronics Engineering Department,*
*TR06531, Ankara-TURKEY*
*e-mail: cadirci@bilten.metu.edu.tr*

**Abstract**

*In this paper, a new approach to demagnetization process of a PWM forward converter (FC) is proposed. According to this approach, the demagnetization winding and diode of a conventional FC are removed, and an external capacitor is added in parallel with the secondary diode. This replacement changes the linear demagnetization process of a conventional FC into a resonant demagnetization process. The theoretical performance results of the proposed resonant demagnetization forward converter (RDFC) are compared with those of a conventional FC. A side by side comparison made between the two types of demagnetization strategies has shown that RDFC has some advantages over FC. The results obtained are also verified experimentally on a prototype 60 W, 333 kHz forward converter.*

## 1. Introduction

The buck-derived conventional PWM forward converter (FC) shown in Fig.1 is a commonly used switch-mode converter topology at relatively low power applications due to its simplicity and cost advantage. In a conventional FC, it is necessary to demagnetize the transformer core during the off time of the main switching element in order to avoid core saturation owing to the flux walking phenomenon. Some additional windings and circuits have been used widely in order to prevent core saturation and limit the voltage stress imposed on the switching element [1-3].

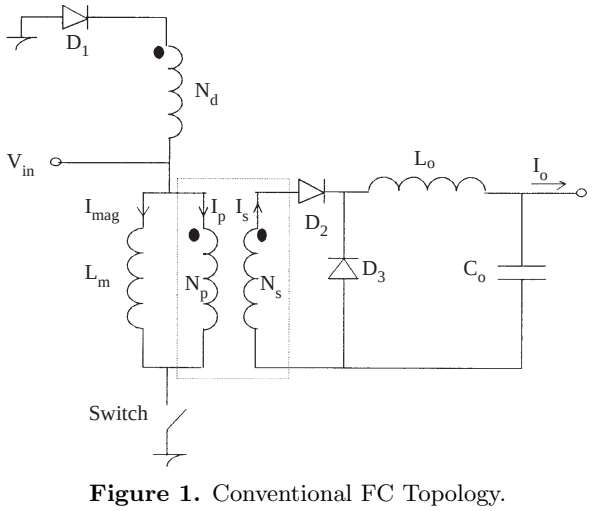


**Figure 1.** Conventional FC Topology.

When the operating frequency is relatively high, such as 500 kHz, or more, demagnetization of the transformer core can be achieved resonantly by the use of parasitic elements [4]. In this approach, the magnetizing inductance of the transformer, and parasitic capacitances of switching devices form a parallel tuned circuit across the transformer. Relationships between these device parameters, and transformer demagnetization time have been derived using exact analytical expressions of FC currents and voltages at all possible operating states [4].

One of the major drawbacks of demagnetizing the transformer core resonantly, by the use of parasitic elements is that parasitics are effective only at relatively high switching frequencies. Furthermore, parasitic capacitance values largely depend on power semiconductor devices used in the circuitry, and on the operating voltage level. Consequently, the control of corresponding parasitic oscillations is rather difficult.

In this paper, a different approach to the demagnetization process of a conventional FC is proposed and analysed. The demagnetization diode and demagnetization winding of an FC (Figure 1) are removed and an external capacitance $C_{ex}$ in parallel with the secondary diode of a conventional FC (Figure 2) is added to control the demagnetization of the transformer. By connecting $C_{ex}$ across the secondary diode D1 in Figure 2 instead of the main switch, $C_{ex}$ is made to deliver its stored energy back to the magnetizing inductance of the transformer without causing extra power dissipation. A resonant demagnetization is hence obtained instead of the linear demagnetization of an FC. Hence, this topology is called a "Resonant Demagnetization PWM Forward Converter" (RDFC). The performance of an RDFC is analyzed theoretically in comparison with a conventional FC. The effects of all parasitic capacitances, the externally added secondary capacitance and leakage inductance of the transformer on the RDFC waveforms are investigated. The results obtained are then verified experimentally on a prototype 60 W converter operating at 333 kHz.

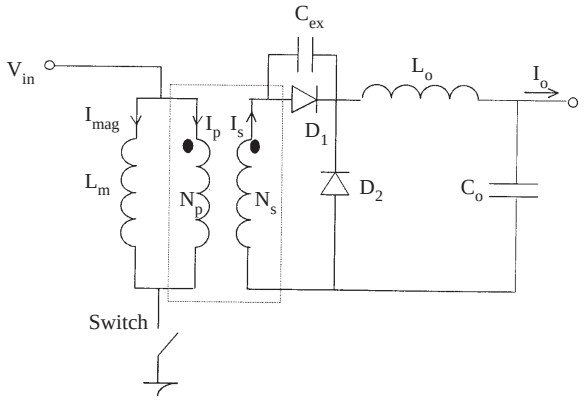


**Figure 2.** RDFC Topology.

# 2. Resonant Demagnetization Forward Converter (RDFC)

## *A. Magnetization and Demagnetization Processes in RDFC*

A switching period of a conventional FC can be divided into three periods. These are the magnetization period (t1), the demagnetization period (t2) and the idle period (t3), as shown in Figure 3.

During the switch-on period, energy is transferred from the input to the output of the transformer. This operation period is called the magnetization period in which the transformer is magnetized with a ramp current, as illustrated in Figure 3. At the end of this period, the current through the magnetizing inductance can be calculated as follows:

$$I_{mag}(t) = (1/L_m) \int_0^{t_{on}} V_{in} dt \Rightarrow I_{mag}(t1) = V_{in}.t_{on}/L_m \quad (1)$$

Since the core has moved in one direction on its hysteresis loop during the magnetization process, it must be exactly restored to its original position before it moves in the same direction in the next cycle to prevent the core from being pushed towards saturation by the flux walking phenomenon [1-3]. This is achieved during the demagnetization period, where the switch is off and there is no energy transfer from input to output. During this off-period of the switch, the FCs transformer is demagnetized by the help of a third winding coupled to the primary called the demagnetization winding and a demagnetization diode. To give enough time for the demagnetization process, the maximum duty cycle of the switch is usually limited to 50% and maximum off-state voltage across the switching element to $2V_{in}$.

Throughout this demagnetization period, energy stored in the transformer is completely given back to the input supply through the demagnetization winding until the transformer is completely demagnetized (t = t2). Since the transformer is demagnetized with a ramp current waveform, the general demagnetization current expression in (2) can be derived using the initial condition $I_{dmag}(t1)=I_{mag}(t1)$.

$$I_{dmag}(t) = I_{mag}(t1)(N_p/N_d) - V_{in}.t/(L_m(N_d/N_p)^2) \quad (2)$$

where $N_p$ and $N_d$ are the number of turns of the primary and demagnetization windings, respectively.

During the idle period, the transformer is completely demagnetized and D1 is in the off state. Output power is supplied by the LC filter. Main waveforms illustrating the operating principles of a conventional FC are given in Figure 4.

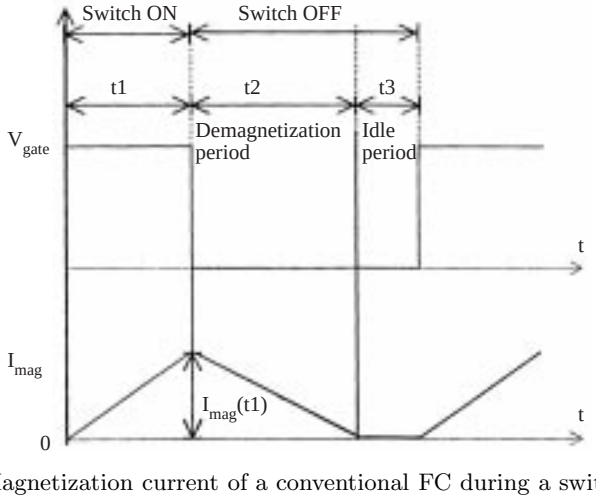


**Figure 3.** Magnetization current of a conventional FC during a switching period.

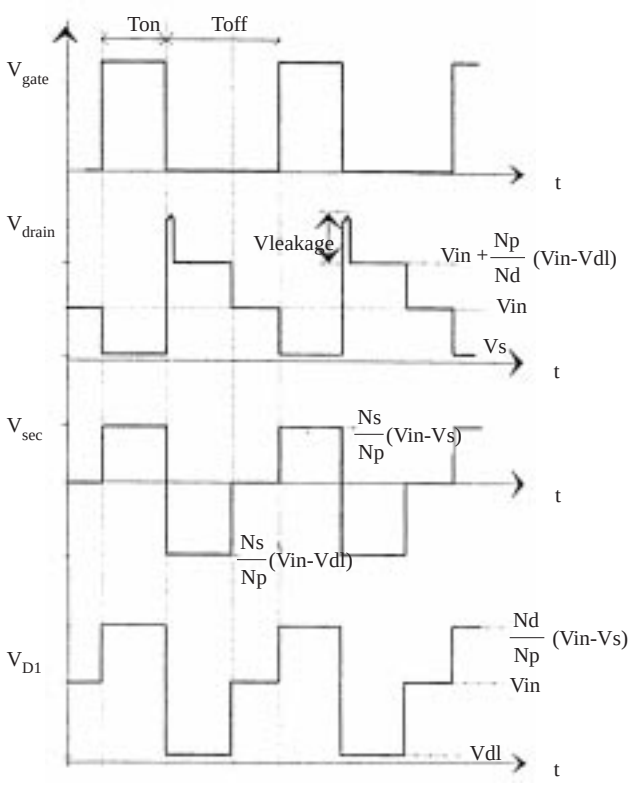


**Figure 4.** Conventional FC waveforms.

The magnetization current of the FC during one switching cycle is unidirectional, as illustrated in Figure 3, and therefore the B-H characteristics of the FC transformer remain in the first quadrant. This may be considered one of the major drawbacks of FCs in some applications where the magnetic operating point is selected near the saturation region, to minimize transformer size.

## *B. Magnetization and Demagnetization Processes in RDFC*

The analysis of the RDFC is carried out first by ignoring the effects of all parasitic elements, assuming that externally added diode capacitance is larger than parasitic capacitances. The magnetization and demagnetization of RDFC transformer is achieved in the following way. First, the transformer is magnetized with a ramp current, as in a conventional FC during the switch-on period. During this period, the secondary current flows through the secondary diode and voltage across the external capacitance is approximately zero. The circuit conditions for this period are given in Figure 5a.

When the switch is turned-off, drain-to-source voltage of the switch rises suddenly to $V_{in}$. When the switch voltage tends to exceed $V_{in}$, the secondary diode D1 turns off, and the freewheeling diode D2 becomes on as seen in Figure 5b. Beyond this point, a sinusoidal demagnetization current starts to flow through the resonance circuit formed by the parallel combination of transformer magnetizing inductance $L_m$, and the external capacitance, $C_{ex}$. $C_{ex}$ charges resonantly from zero to a peak value of $I_m$ $(L_m/C_{ex})^{1/2}$ in the polarity shown in Figure 5b, and then discharges back to zero. The resonative demagnetization current, and external capacitance charging voltage equations during the switch OFF period with D1 OFF, and D2 ON can be written as follows:

Since $i_{dmag}(0) = I_m$, $di_{dmag}(0)/dt = 0$, and $v_{Cex}(0) = 0$;

$$i_{dmag}(t) = I_m \cos w_c(t); v_{Cex}(t) = I_m(L_m/C_{ex})^{1/2} \sin w_c(t) \quad (3)$$

where $w_c = 1 / (L_m\ n^2 C_{ex})^{1/2}$ and, $I_m = V_{in}\, t_{on} / 2L_m$

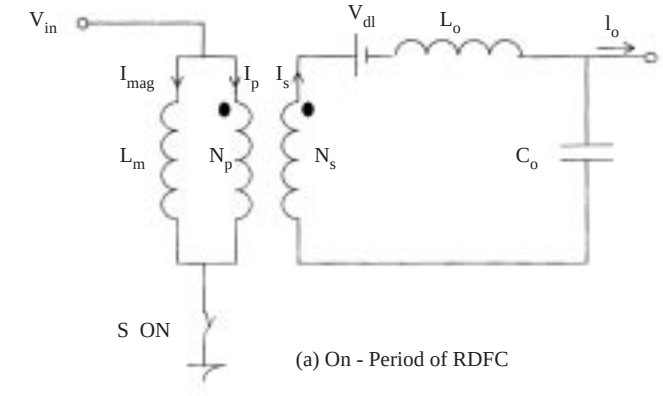


(a) On - Period of RDFC

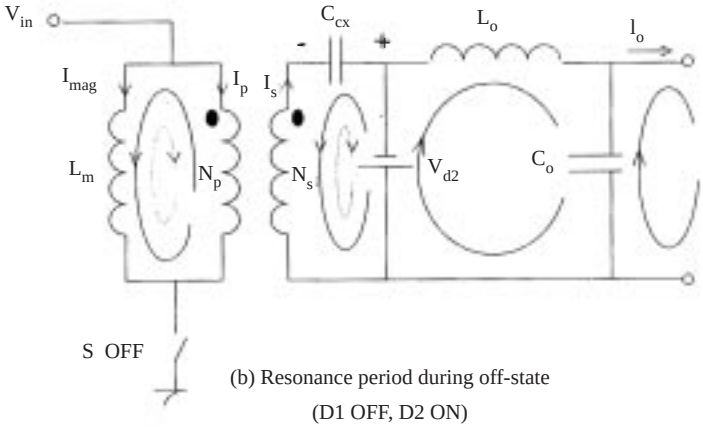


(b) Resonance period during off-state
(D1 OFF, D2 ON)

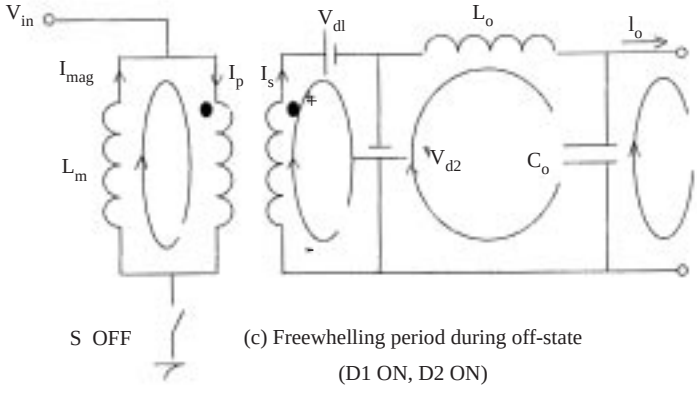


(c) Freewhelling period during off-state
(D1 ON, D2 ON)

**Figure 5.** Circuit conditions of RDFC at switch-on/off periods.

The sinusoidal current continues to magnetize the transformer in the reverse direction until the switch voltage drops resonantly back to $V_{in}$ and the voltage across the external capacitance tends to exceed zero, where secondary diode D1 becomes on again (Figure 5c). The magnetizing current then remains constant

at the negative peak value (-$I_m$) and circulates in the secondary loop formed by D1 and the freewheeling diode D2 until the beginning of the next switch-on period.

It is worth noting that $C_{ex}$ in parallel with D1 does not cause extra power dissipation since it delivers the energy stored at the beginning of resonance back to magnetizing inductance at the end of resonant demagnetization. An external capacitance connected in parallel with the main switch (MOSFET) could also be used for the same resonant demagnetization process, but this would occur at the expense of a considerable amount of extra power dissipation ($^1/_2$ $C_{ex}$ $V^2$ $f_{sw}$) during the turn-on time of power MOSFET.

### *C. Spice Simulation Results*

The simulation of a sample RDFC whose design specifications are given in Appendix A is carried out using the Spice simulation program, and the corresponding drain voltage and magnetization current waveforms are given in Figure 6. It can be observed from these waveforms that as the voltage across the switch reaches the value of $V_{in}$, magnetizing inductance resonates with $C_{ex}$ and all the magnetization current flows through secondary side of transformer.

### *D. Effects of Parasitic Capacitance, Transformer Leakage Inductance and $C_{ex}$ on RDFC Performance*

In the RDFC, the major parasitic elements of the FC contribute to the demagnetization process. These are

- leakage inductance of transformer;
- output capacitance of switching element;
- parasitic capacitance of secondary diode; and,
- transformer parasitic capacitances.

During the switch-off period, since the secondary diode turns off, as the drain voltage tends to exceed $V_{in}$, the equivalent circuit on the primary side becomes as shown in Figure 7. This circuit can be assumed to have two different resonance frequencies. The main resonance phenomenon, used in the demagnetization of transformer will take place at a lower frequency. This occurs between the magnetizing inductance $L_m$ and the parallel combination of externally connected capacitance $C_{ex}$, with the parasitic capacitances of the switch $C_s$, and secondary diode ($C_{os}$).

Parasitic resonance occurs at much higher frequency. It takes place between the leakage inductance of the transformer and the series combination of parasitic MOSFET and diode capacitances with $C_{ex.}$ Such high frequency resonance is undesirable because it is a source of EMI.

The associated low and high resonance frequencies can be determined as follows: assuming that $L_{leak}$ is much smaller than $L_m$ in Figure 7, the parallel combination of $C_d$ snd $C_s$ resonates with $L_m$ giving the low frequency resonance component

$$Z_{rl} = [L_m/(C_d + C_s)]^{1/2}, w_{cl} = 1/[L_m(C_d + C_s)]^{1/2} \tag{4}$$

The magnetizing reactance can be assumed infinitely large for the determination of the high frequency resonance component. This assumption leads to a new circuit in which $L_{leak}$ resonates with the series combination of $C_d$ and $C_s$.

$$Z_{rh} = [L_{leak}(C_d + C_s)/C_dC_s]^{1/2}, w_{ch} = [1/L_{leak}C_dC_s/(C_d + C_s)]^{1/2} \tag{5}$$

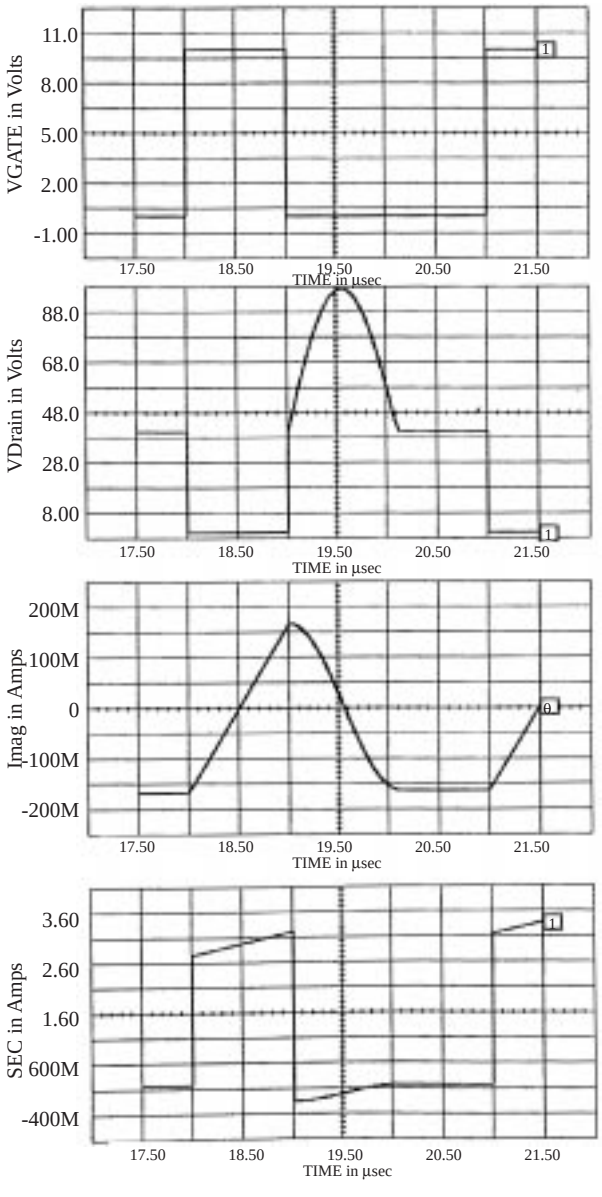


**Figure 6.** Waveforms of RDFC with Cex only.

High frequency resonance component damps out within a few cycles because energy stored in leakage inductance is lost on the transformer and wire resistances. The spice simulation circuit of the 60 W, RDFC switched at 333 kHz (see Appendix A for design specifications) and the corresponding results taking into account of all parasitics are given in Figures 8 and 9, respectively. Effects of different secondary capacitance values ($C_{eq}$) on the frequency of parasitic resonance are as given in Appendix B.

The transformer magnetizing inductance has no effect on parasitic resonance as far as its frequency ($\approx$30 MHz for the sample RDFC) is much higher than that of demagnetization resonance ($\approx$1MHz). The dominating capacitance in the parasitic resonance depends on various circuit parameters such as the supply size, circuit layout, semiconductor type and operating voltage. The variations in the output capacitances of semiconductors with the bias voltage are given in Appendix C for the FC and RDFC designed and implemented within the scope of this study.

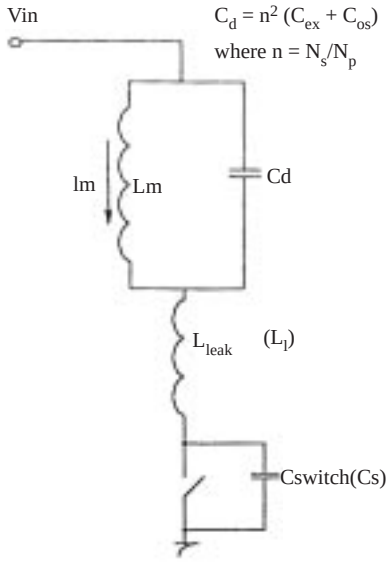


**Figure 7.** Primary equivalent circuit of RDFC with parasitics.

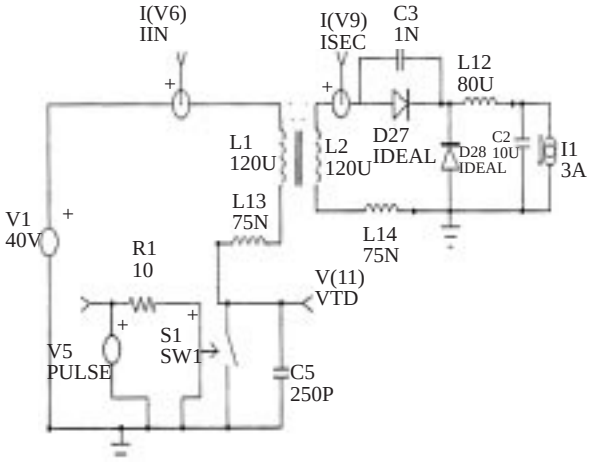


**Figure 8.** Spice simulation circuit of RDFC with all parasitics.

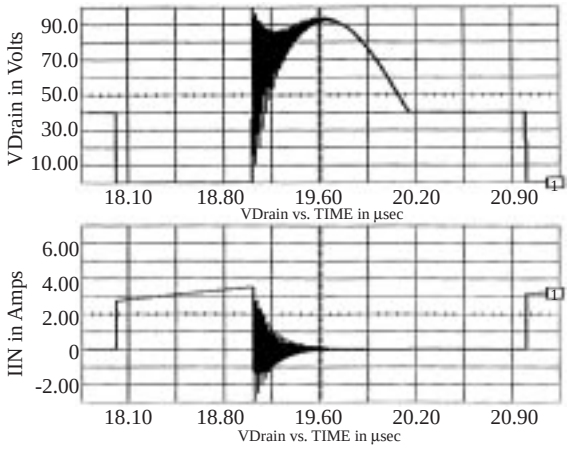


**Figure 9.** Spice simulation results of circuit in Figure 8.

# 3. Comparison of RDFC and FC

The FC and RDFC have been designed for the same input-output specifications, and implemented on identical PCBs in order to allow an experimental comparative study. The characteristic waveforms of an RDFC, such as drain-to-source voltage of MOSFETs and secondary voltages are obtained for various operating conditions, and are then compared with theoretical ones.

A typical set of waveforms for the RDFC and FC is given in Figure 10. In general, good agreement has been obtained between the experimental and Spice simulation results. An examination of drain-to-source voltage waveforms shows that in the experimental set-up, the parasitic resonance damps out in a shorter time as compared to simulation results. This is attributed to the fact that damping due to resistance of the core material is ignored in Spice simulation of converters. However, this phenomenon affects the performance of converter switches at parasitic resonance frequencies (≈30 MHz).

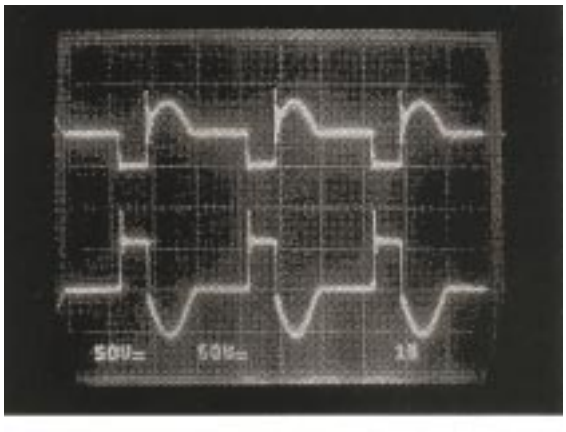

i-RDFC

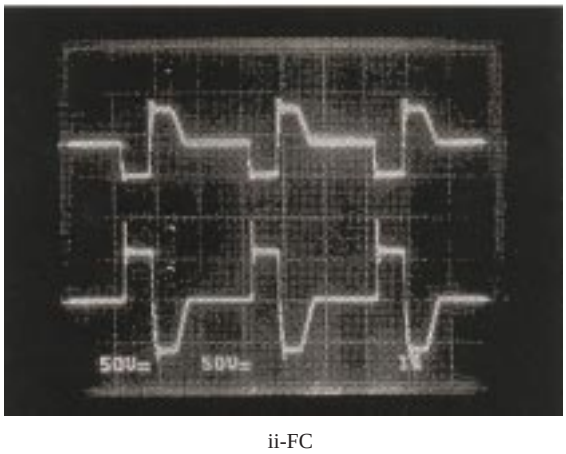

ii-FC

**Figure 10.** Experimental drain and secondary voltages of i- RDFC and ii- FC at $V_{in} = 40$ V, $I_o$=2.5 A.

## *A. Performance Calculation*

As can be observed from the experimental drain voltage waveforms given in Figure 10, RDFC has a smooth, partly sinusoidal drain voltage waveform with constant amplitude whereas the FCs drain voltage waveform is clamped at $2V_{in}$, and has sharper edges. In a PWM-SMPS topology, it is advantageous to have a low

off-state voltage stress across the switching element, and a wide duty cycle range to regulate over a wider input voltage range. In this section, a comparative study is performed between conventional FC and RDFC based on these objectives.

In practice, the FC's duty cycle is usually limited to 0.5 . Therefore, a comparison between FC and RDFC is made by assuming that the maximum duty cycle is 0.5, and the demagnetization period is equal to half of the switching period ($0.5\ T_{sw}$) at $V_{in(min)}$ for both converters. Then the RDFC has a constant resonance period ($T_{res} = 0.5\ T_{sw}$), and resonance peak voltage $V_p$ as given in Equation 6.

$$V_p = \frac{V_{in}T_{on}}{2L_m}(L_m/C_{eq})^{1/2} \quad ; \quad T_{res} = \pi(L_mC_{eq})^{1/2} \tag{6}$$

At $V_{in(\min)}, T_{res} = T_{onmax} = \pi(L_mC_{eq})^{1/2} \Rightarrow V_p = \pi/2V_{in(\min)}$

At maximum input voltage, the FC will have a peak off-state drain voltage of $2V_{in(max)}$ . However, in the RDFC, if input voltage range meets the constraint in Equation 7, the resonance peak value $V_p$ is less than $V_{in(max)}$, resulting in a voltage stress across the switch ($V_{peak}$=$V_p$+$V_{in(max)}$) lower than that of the FC when both of them have equal demagnetization periods ($0.5T_{sw}$) at $V_{in(min)}$.

$$V_{in(\max)}/V_{in(\min)} \geq \pi/2 \tag{7}$$

A comparison between an FC and RDFC can also be made by assuming that the maximum value of peak off-state drain voltage ($V_{peak}$) to which the switches are subjected is nearly the same for both converters. Let $V_{peak} = 2V_{in(\max)}$. This can be maintained in the RDFC by setting the peak resonance voltage magnitude to nearly $V_{in(max)}$. For the FC, however, maximum duty cycle must be limited to 0.5 to satisfy this condition when the main winding and the demagnetization winding have an equal number of turns ($N_p = N_d$). For the above design specifications, the input voltage regulation range is measured at full load for both converters. It is observed that the designed RDFC can regulate over a wider input voltage range of 17-45 V with a maximum duty cycle of 0.63, whereas the FC does not have enough time for demagnetization below $V_{in} = 20$ V with a duty cycle limited to 0.5. In general, an RDFC has a more flexible design since it permits a compromise between the maximum allowable off-state voltage across the switch and the supply's regulation range by changing the value of $C_{ex}$ accordingly.

The efficiency of the FC and RDFC are also measured for various input voltage and output current values and the corresponding results are given in Table 1. RDFC is slightly more efficient than FC due to the removal of the demagnetization winding and diode.

**Table 1.** Efficiency of RDFC and FC for different $V_{in}$ and $I_o$.

| | Efficiency, % | | | | | |
|---|---|---|---|---|---|---|
| | $V_{in}$ = 20V | | $V_{in}$ = 28V | | $V_{in}$ = 40V | |
| $I_o$, A | RDFC | FC | RDFC | FC | RDFC | FC |
| 1.0 | 83.4 | 82.9 | 81.9 | 81.6 | 79.0 | 78.4 |
| 2.0 | 86.5 | 85.0 | 86.5 | 85.8 | 84.4 | 84.0 |
| 5.0 | 80.5 | 80.0 | 81.6 | 80.6 | 81.7 | 81.5 |

### *B. Effects of $C_{ex}$ on Drain Voltage Waveform in RDFC*

The resonance peak voltage value ($V_p$), half of resonance period ($T_{res}/2$) and peak off-state drain voltage ($V_{peak}$) variations with respect to the externally added capacitance are measured and the corresponding results are reported in Table 2. It is observed from these results that as $C_{ex}$ is increased $V_p$ decreases, whereas $T_{res}$ increases.

**Table 2.** $C_{ex}$ vs. drain voltage parameters.

| $C_{ex}$, pF | $V_p$, V | $T_{res}$, $\mu$sec | $V_{peak}$, V |
|---|---|---|---|
| 270 | 43.8 | 0.93 | 74.3 |
| 470 | 36.6 | 1.07 | 68.5 |
| 560 | 35.4 | 1.09 | 66.8 |
| 1000 | 29.7 | 1.32 | 60.2 |
| 1500 | 24.7 | 1.54 | 56.6 |
| 2700 | 21.3 | 1.83 | 52.1 |

### *C. Qualitative Evaluation of Demagnetization Methods*

In the sample RDFC switched at 333 kHz, the equivalent parasitic capacitance of the switching devices and transformer referred to the secondary side ($C_{eq} \approx 600$ pF) become comparable to externally added capacitance value ($C_{ex} = 560$ pF). Therefore, at higher switching frequencies, parasitic capacitance is the dominating capacitance. At lower frequencies, however, $C_{ex}$ dominates.

A qualitative examination of demagnetization methods applicable to forward converters can be made by using the experience gained in the design of conventional FCs, and by carrying out several preliminary design works for RDFCs in relatively low power applications, and for practical input and output voltage ranges. These results are summarized qualitatively in Table 3 for low, medium, and high frequency ranges.

**Table 3.** Demagnetization methods vs. frequency.

| | Demagnetizing winding | **Only** parasitics | External $C_{ex}$ |
|---|---|---|---|
| LF | √ | - | √ |
| MF | √ | may be effective | √ |
| HF | - | √ | - |

LF: Low frequency range: $f_{sw} \leq 100$ kHz
MF: Medium frequency range: $f_{sw}$:100–500 kHz
HF: High frequency range: $f_{sw} \geq 500$ kHz.

## Conclusions

A comparison made between the two topologies having the same control strategy and operating under the same input/output conditions shows that the RDFC has a smooth, partly sinusoidal, constant-peak drain voltage, whereas the FC has a stepped drain voltage clamped at $2\,V_{in}$. The RDFC can be designed to have a shorter demagnetization period at $V_{in(min)}$, and a lower drain off-state voltage at $V_{in(max)}$ given that $V_{inmax}/V_{inmin} \geq \pi/2$. It has a wider regulation range than the FC. The RDFC is slightly more efficient than the conventional FC due to the removal of the demagnetization diode, and demagnetization winding

of the transformer. An RDFC transformer has bidirectional B-H characteristics unlike an FC, which has a unidirectional one. This brings an advantage to the RDFC, especially interms of core size minimization. The RDFC has a lower implementation cost than the conventional FC. The planar transformer technology can be more easily implemented in RDFC topology due to the removal of demagnetization winding. The use of planar transformer technology would minimize volume and weight, and further increase efficiency.

# Appendices

## *A. Basic design specifications of FC and RDFC*

| | |
|---|---|
| Minimum input voltage, | $V_{in(min)} = 17$ V |
| Maximum input voltage, | $V_{in(max)} = 45$ V |
| Minimum output current, | $I_{omin} = 0.5$ A |
| Maximum output current, | $I_{omax} = 5$ A |
| Output voltage, | $V_{out} = 12$ V |
| Switching frequency, | $f_{sw} = 333$ kHz |
| Efficiency, | $\eta \geq 0.8$ |
| Maximum output ripple, | $V_{rip} \leq 50$ mV |

## *B. Parasitic Resonance Frequency vs $C_{eq}$*

**Table 3.** $C_{eq}$ vs. Leakage Resonance Frequency.

| $C_{eq}$, pF | $F_{r-leak}$, MHz |
|---|---|
| 0 | 36.7 |
| 220 | 31.8 |
| 330 | 29.8 |
| 560 | 28.8 |
| 1000 | 27.9 |
| 2700 | 26.9 |

## *C. Variations of switch output capacitances with bias*

**Table 4.** MOSFET (IRF530) output capacitance against bias voltage.

| Bias voltage, V | Output capacitance $C_s$, pF |
|---|---|
| 0 | 2250 |
| 10 | 490 |
| 30 | 293 |
| 50 | 230 |
| 70 | 195 |

**Table 5.** Schottky diode (MBR10100) output capacitance.

| Bias voltage, V | Output capacitance $C_{os}$, pF |
|---|---|
| 0.1 | 966 |
| 1 | 793 |
| 5 | 391 |
| 10 | 286 |
| 30 | 178 |
| 60 | 139 |

### *D. Transformer inductances and parasitic capacitances*

| | |
|---|---|
| Primary leakage inductance, | $L_{leakp} = 50$ nH |
| Secondary leakage inductance, | $L_{leaks} = 110$ nH |
| Magnetizing inductance, | $L_m = 45\mu$H |
| Primary interwinding capacitance, | $C_p = 4$pF |
| Secondary interwinding capacitance, | $C_{sec} = 6$pF |
| Primary to secondary capacitance, | $C_{ps} = 220$pF |

### *E. Photograph of designed FC and RDFC*

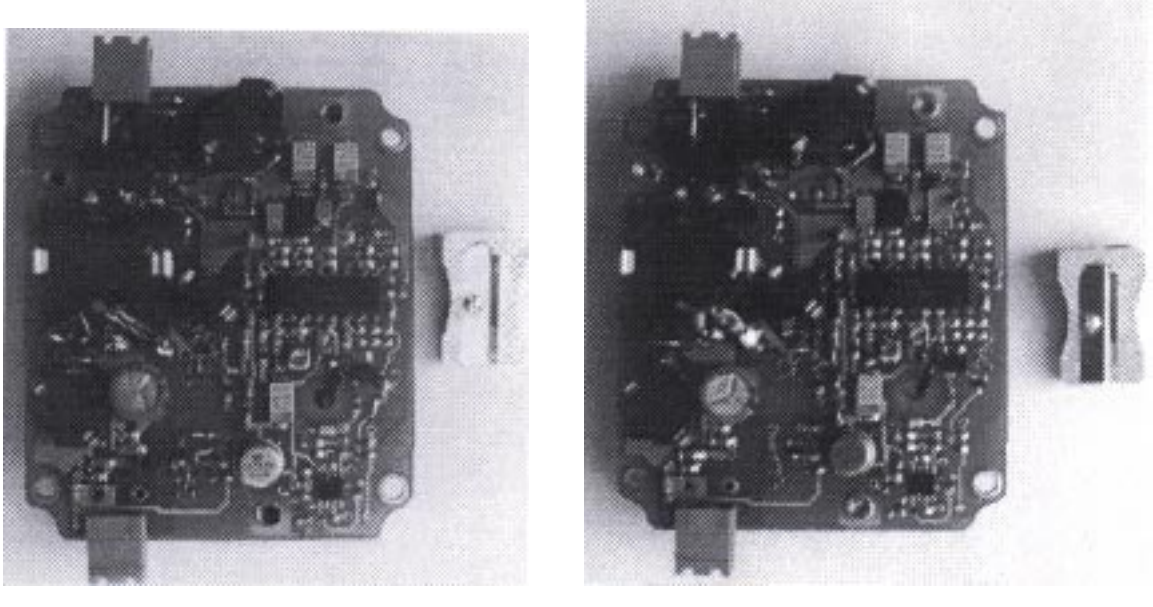

On the left Photograph: FC

On the right Photograph: RDFC

## References

[1] M. Brown, "Practical Switching Power Supply Design", Academic Press, USA, 1990.

[2] A.I. Pressmann, "Switching Power Supply Design", McGraw Hill, 1991.

[3] R.P. Severns, and G. Bloom, "Modern DC-to-Dc Switchmode Power Converter Circuits", Van Nostrand Reinhold, 1984.

[4] N. Murakami and M. Yamasaki, "Analysis of a Resonant Reset Condition for a Single Ended Forward Converter", IEEE PESC'88 Record, April 1988, pp.1018-1023.

[5] N. Mohan, T.M. Undeland, W.P. Robbins, "Power Electronics: Converters, Applications, and Design", John Wiley and Sons, $2^{nd}$ Ed., pp. 311.